2010 IEEE International Conference on Robotics and Automation
Anchorage Convention District
May 3-8, 2010, Anchorage, Alaska, USA

A new device dedicated to autonomous mobile robot dynamic stability: Application to an off-road mobile robot

Nicolas Bouton◇, Roland Lenain◇, Benoit Thuilot⋆ and Philippe Martinet⋆

Abstract— **Automation in outdoor applications (farming, surveillance, etc.) requires highly accurate control of mobile robots, at high speed, accounting for natural ground specificities (mainly sliding effects). In previous work, predictive control algorithms dedicated to All-Terrain Vehicle lateral stability was investigated. Satisfactory advanced simulation results have been reported but no experimental ones were presented. In this paper, the prevention of a real off-road mobile robot rollover is addressed. First, both rollover dynamic modeling and previous work on a *Mixed observer* designed to estimate on-line sliding phenomena for path tracking control are recalled. Then, this observer is here used to compute a rollover indicator accounting for sliding phenomena, from a low-cost perception system. Next, the maximum vehicle velocity, compatible with a safe motion over some horizon of prediction, is computed via Predictive Functional Control (PFC), and can then be applied, if needed, to the vehicle actuator to prevent from rollover. The capabilities of the proposed device are demonstrated and discussed thanks to real experimentation.**

I. INTRODUCTION

Off-road mobile robots appear as an interesting solution so as to answer social needs in various fields of application ([17] - farming, surveillance, military activities, etc). However, if many potential devices can take benefits of innovation in this area (increasing work accuracy, decreasing the level of risk), such applications require highly accurate control laws, able to preserve vehicle stability even at high speed. Indeed, in off-road mobile robot context, the complexity and the variability of the encountered phenomena have to be tackled to ensure both accuracy and security. Nevertheless, if numerous systems have been developed for road vehicles (active suspensions, active steering [2], steering and braking control [1] and [16]), they appear to be poorly relevant for fast off-road motion context (since they do not adapt to varying grip conditions). Consequently, specific safety devices have to be designed for off-road mobile robots.

The first step in the development of such devices is the design of a rollover indicator dedicated to off-road mobile robots. Previous work [5] has shown that the Lateral Load Transfer (*LLT* - [6]) is a very relevant criterion. Its advantages, with respect to other stability metrics such as the Static Stability Factor (SSF) [10], the force-angle measurement criterion [12] or the Zero Moment Point (ZMP - proposed usually to investigate humanoid and mobile robot stability, [15]) are that, on the one hand it does not demand for a huge and expensive perception system, and on the other hand it is not dependent on some thresholds particularly difficult to tune in outdoor environment.

In order to use properly such a metric in an off-road context, grip conditions have to be known. A new observer has been proposed in [8]. It consists in the on-line adaptation of tire cornering stiffnesses, representative of grip conditions, based on a vehicle dynamic model. Then, using the adapted parameters, it permits to access the sideslip angles to be entered into the algorithms proposed in [7], so as to control robot motion with a high accuracy whatever ground conditions, vehicle velocity (up to 40km/h) and the shape of the path to be followed. Thanks to the estimation of cornering stiffnesses, this observer appears also to be relevant in the on-line computation of the Lateral Load Transfer and finally for the design of stabilizing algorithms.

In this paper, this indicator is used as a basis for designing an active anti-rollover device dedicated to mobile robots. More precisely, the maximum vehicle velocity ensuring that the *LLT* remains within a safety range over the horizon of prediction is estimated on-line, and can then be applied to the vehicle actuator in order to avoid imminent rollover. The algorithm relies on Predictive Functional Control principle (PFC - [14], [19]), so that off-road mobile robot dynamic features can be accounted.

The paper is organized as follows: vehicle modeling in presence of slidings used to develop the control device is presented. Then, previous work on path tracking is recalled as well as the notion of *Mixed observer* used for the estimation of grip conditions (cornering stiffnesses) and sliding parameters (sideslip angles). Next, Predictive Functional Control principle is applied to design vehicle velocity control law in order to guarantee lateral dynamic stability of mobile robots on slippery ground. Finally, experimental results are reported to validate the relevancy of the proposed approach in situations where lateral rollover is imminent.

II. VEHICLE DYNAMIC MODELING

A. Vehicle dynamic model

In order to describe the rollover of a mobile robot, its motion in yaw and roll representations has to be known. Then, two representations are here introduced: one is a yaw representation (Fig.1(a)) (also used to develop the *Mixed observer* described in Section III-B) and the other one is a roll representation (Fig.1(b)). The yaw model, also used for path tracking and sliding estimation (see III-B) aims at describing the overall vehicle motion on the ground and consists of an extended bicycle model of the mobile robot.

◇ Cemagref, 24 av. des Landais, BP 50085, 63172 Aubière Cedex, France
nicolas.bouton and roland.lenain@cemagref.fr
⋆ LASMEA, 24 avenue des Landais , 63177 Aubière Cedex, France
benoit.thuilot and philippe.martinet@lasmea.univ-bpclermont.fr

It is used to estimate some vehicle motion variables (as the lateral acceleration of the vehicle center of gravity) and sideslip angles. These variables are then injected into the second part of the dynamic model, characterized by a roll 2D projection (shown on Fig.1(b)), used to compute roll angle, roll rate and the *LLT*.

The notations used in this paper, and reported in Fig.1(a) and Fig.1(b), are listed below:

- $R_0(x_0, y_0, z_0)$ is the frame attached to the ground,
- $R_1(x_1, y_1, z_1)$ is the yaw frame attached to the vehicle,
- $R_2(x_2, y_2, z_2)$ is the roll frame attached to the suspended mass,
- ψ is the vehicle yaw angle,
- φ_v is the roll angle of the suspended mass,
- δ is the steering angle,
- β, α_r, α_f are the global, rear and front sideslip angles,
- v is the linear velocity at the center of the rear axle,
- u is the linear velocity at the roll center,
- a and b are the front and rear vehicle half-wheelbases,
- $L = a + b$ is the vehicle wheelbase,
- c is the vehicle track,
- h is the distance between the roll center O' and the vehicle center of gravity G,
- I_x, I_y, I_z are the roll, pitch and yaw moments of inertia,
- $P = mg$ is the gravity force on the suspended mass m, with g denoting the gravity acceleration,
- F_f and F_r are the front and rear lateral forces,
- F_{n1} and F_{n2} are the normal component of the tire/ground contact forces on the vehicle left and right sides,
- F_a is a restoring-force parametrized by k_r and b_r, the roll stiffness and damping coefficients:

$$\overrightarrow{F_a} = \frac{1}{h}\left(k_r\varphi_v + b_r\dot{\varphi}_v\right)\overrightarrow{y_2} \tag{1}$$

The roll stiffness k_r and the distance h are assumed to be preliminary calibrated ([3]). The roll damping b_r is experimentally evaluated (through a driving procedure) and the other parameters (wheelbase, weight, etc) are directly measured. The velocity v, the steering angle δ and the yaw rate $\dot{\psi}$ are measured using respectively a Doppler radar, a steering angle sensor and a gyrometer as mentioned in Section V. Finally, the velocity v is also considered as the control variable of the anti-rollover device and the steering angle δ is the path tracking control variable.

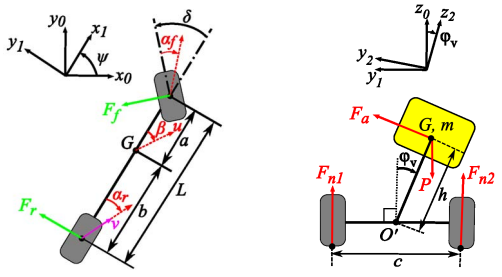

(a) Yaw projection. (b) Roll projection.

Fig. 1. Vehicle modeling.

B. Motion equations

Motion equations issued from the yaw projection shown in Fig.1(a) require analytical expressions of lateral forces F_f and F_r. Therefore, as explained in [4], a simple linear tire model has been considered. It can be expressed as:

$$\left\{\begin{array}{rcl} F_f &=& C_f(.)\alpha_f \\ F_r &=& C_r(.)\alpha_r \end{array}\right. \tag{2}$$

This model requires only the knowledge of α_f and α_r, defined in (3), and the front and rear cornering stiffnesses $C_f(.)$ and $C_r(.)$ supposed to be slow varying. In order to reflect the variable grip conditions, these two parameters are on-line estimated thanks to the *Mixed observer* detailed in Section III-B. Only one parameter is then needed, contrary to classical tire models such as the celebrated Magic formula [11].

Based on (2), the dynamic equations of the yaw model (see [18]) can be expressed as:

$$\left\{\begin{array}{rcl} \ddot{\psi} &=& \frac{1}{I_z}\left(-aC_f\alpha_f\cos(\delta) + bC_r\alpha_r\right) \\ \dot{\beta} &=& -\frac{1}{um}\left(C_f\alpha_f\cos(\beta-\delta) + C_r\alpha_r\cos(\beta)\right) - \dot{\psi} \\ \alpha_r &=& \arctan\left(\tan(\beta) - \frac{b\dot{\psi}}{u\cos(\beta)}\right) \\ \alpha_f &=& \arctan\left(\tan(\beta) + \frac{a\dot{\psi}}{u\cos(\beta)}\right) - \delta \\ u &=& \frac{v\cos(\alpha_r)}{\cos(\beta)} \end{array}\right. \tag{3}$$

C. Lateral Load Transfer computation

1) LLT definition: The general expression of the Lateral Load Transfer (*LLT*) (see [9], [1]) is:

$$LLT = \frac{F_{n1} - F_{n2}}{F_{n1} + F_{n2}} \tag{4}$$

Clearly, a rollover situation is detected when a unitary value of $|LLT|$ is reached, since it corresponds to the lift-off of the wheels on the same side of the vehicle. Here, the vehicle behavior will be considered as hazardous when *LLT* reaches the critical threshold LLT_{limit} ($|LLT| \leq LLT_{limit}$).

2) LLT dynamic equations: In order to extract normal force expressions from the roll model (see Fig.1(b)), the following assumptions have been made:

- The entire vehicle mass is suspended, which implies insignificant non-suspended mass (essentially tires),
- The suspended mass is assumed to be symmetrical with respect to the two planes (z_2, y_2) and (x_2, z_2). The inertial matrix is then diagonal:

$$I_{G/R_2} = \left[\begin{array}{ccc} I_x & 0 & 0 \\ 0 & I_y & 0 \\ 0 & 0 & I_z \end{array}\right] \tag{5}$$

- Sideslip angles α_f, α_r and β are assumed to be small (corroborated by experiments),
- As a consequence, the vehicle velocity u at roll center can be considered to be equal to the rear axle one (i.e. $u \approx v$), see (3).

Using these assumptions, the *LLT* indicator can be evaluated from the Newton Euler formalism applied to the overall

system, subjected to four external forces (P, F_a, F_{n1} and F_{n2}). More precisely, variations of φ_v, F_{n1} and F_{n2} can be derived as:

$$\ddot{\varphi}_v = \frac{1}{h\cos(\varphi_v)}[h\dot{\varphi}_v{}^2\sin(\varphi_v) + h\dot{\psi}^2\sin(\varphi_v) + u\dot{\psi}\cos(\beta) + \dot{u}\sin(\beta) + u\dot{\beta}\cos(\beta) - \left(\frac{k_r\varphi_v + b_r\dot{\varphi}_v}{mh}\right)\cos(\varphi_v)] \quad (6)$$

$$F_{n1} + F_{n2} = m\left[-h\ddot{\varphi}_v\sin(\varphi_v) - h\dot{\varphi}_v{}^2\cos(\varphi_v) + g - \left(\frac{k_r\varphi_v + b_r\dot{\varphi}_v}{mh}\right)\sin(\varphi_v)\right] \quad (7)$$

$$F_{n1} - F_{n2} = \frac{2}{c}\left[I_x\ddot{\varphi}_v + (I_z - I_y)\left[\dot{\psi}^2\cos(\varphi_v)\sin(\varphi_v)\right] - h\sin(\varphi_v)(F_{n1} + F_{n2})\right] \quad (8)$$

In order to infer the roll angle and the LLT from (6)-(8), the global sideslip angle and the yaw rate are both required. Since the former one cannot be measured, an observer has been designed and is presented below.

III. Path tracking control

A. Path tracking control principle

Previous work was dedicated to the development of off-road mobile robot path tracking algorithms acting at high speed. The path tracking control law considered makes use of a mixed kinematic and dynamic observer, detailed in Section III-B. Indeed, an extended kinematic model, detailed in [7], consists in adding a limited number of variables (front and rear sideslip angles, respectively denoted α_f and α_r in the modeling section II-A) representative of low grip conditions into a pure kinematic model. The global scheme of the path tracking control law is depicted in Fig. 2 where y and $\widetilde{\psi}$ are respectively the lateral deviation and the angular deviation relative to the path to be followed.

Briefly, it consists in using sliding parameters estimated from the *Mixed observer* (denoted backstepping observer in Fig. 2) and the measurement of both the lateral deviation of the vehicle with respect to the reference trajectory and the orientation of the mobile robot, so as to compute on-line the steering angle of the vehicle which ensures an accurate path tracking. The computation of the control variable is based on predictive and adaptive algorithms, as detailed in [8].

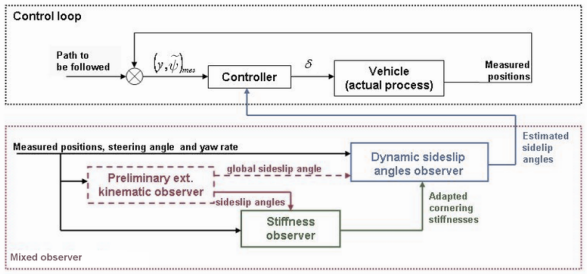

Fig. 2. Scheme of the path tracking controller.

B. Mixed observer for grip condition estimation

As explained in the previous paragraph, both the dynamic modeling used to compute LLT and the path tracking algorithm require an estimation of sliding parameters. Then, an indirect estimation of dynamic model parameters is mandatory. Since appropriate sensors are missing, this is achieved in several steps, using different level of modeling (kinematic and dynamic). This multilevel estimation is gathered in the so called *Mixed observer* detailed in [8]. Its general principle is described in Fig. 2. The observation loop consists of successive steps, each one relying on the variable supplied by the preceding step. The three blocks shown in Fig. 2 are described below:

- A preliminary extended kinematic observer *(red dashed box)* is first used to supply relevant tire sideslip angle estimation at low speed.
- Then, the parameters obtained by the kinematic observer are used in the cornering stiffness observer *(green dotted box)* where the cornering stiffnesses are on-line adapted with the aim of reflecting grip condition variations.
- Finally, with the adapted parameters, a dynamic sideslip angle observer *(blue dashed dotted box)*, derived from standard observer theory, is applied to the dynamic model (3) in order to get relevant sideslip angles estimation at high speed and whatever the grip conditions.

The sliding angle estimates supplied by such an observer are relevant to compute LLT and to develop anti-rollover predictive control laws as detailed below.

IV. Predictive functional control algorithm

A. Strategy of LLT limitation

In order to avoid the rollover risk, the limitation of the LLT (i.e. $|LLT| \leq LLT_{limit}$) through the control of the vehicle speed is here investigated. The idea is to compute at each time the velocity leading to LLT_{limit} one moment in the future. This value can then be considered as the maximum admissible velocity (denoted v_{max} in the sequel) to avoid lateral rollover situation.

The overall scheme is depicted in Fig.3. The path tracking controller permits to ensure the robot navigation (δ is used as the steering angle control variable), when the computation of the maximum velocity, detailed in Section IV-C, and represented by the block "Predictive control" supplies v_{max}. Relying on this variable, the speed limitation process consists then in the following steps:

- The "Min" block supplies the rear axle linear velocity control input v_{input} to be applied to the vehicle. This variable is deduced from the comparison between the velocity desired v_d (a constant velocity is specified at the beginning of the test) and the maximum velocity v_{max}: $v_{input} = \min(v_d, v_{max})$
- The measurements shown in Fig.3 are then used to estimate on-line the sliding parameters and the cornering stiffnesses thanks to the *Mixed observer* described in Section III-B,

- Then, stiffnesses (from the *Mixed observer* detailed in Section III-B), the measured rear axle linear velocity and the measured steering angle are reported into the vehicle roll model in order to compute the roll angle φ_v and the *LLT* (see Section II-C),
- Finally, the roll angle φ_v, the sliding parameters and the steering angle are processed in the "Predictive Control" block in order to supply the maximum velocity v_{max}.

In order to anticipate (and then avoid) hazardous situations, the computation of v_{max} is based on the Predictive Functional Control (PFC) formalism, detailed in [13] and [19]. With this approach, the vehicle velocity is viewed as a control variable and v_{max} is designed in order to ensure the convergence of the *LLT* to the value LLT_{limit}.

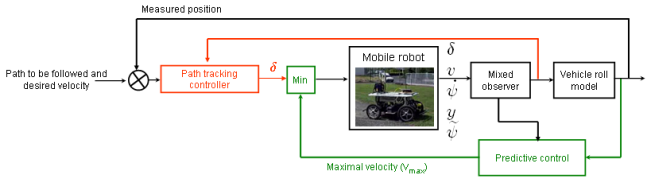

Fig. 3. Velocity control of an autonomous mobile robot.

B. Roll angle model

As it can be seen in equations (7) and (8), the *LLT* does not rely explicitly on vehicle velocity, but on roll angle: vehicle velocity should then be designed to control φ_v.

The roll angle equation (6) is non-linear when PFC formalism requires linear equations, see [14]. Therefore, as a first step, it is necessary to approximate equation (6) to a linear model. In the sequel, φ_{vNL} and φ_{vL} denote the roll angle supplied respectively by non-linear model (6) and by the linear model to be derived.

In order to achieve the linearization, the following assumptions are considered:

- Sideslip angles are quite small and consequently, based on (3), the vehicle yaw rate can be approximated by:

$$\dot{\psi} = u\left(\frac{\delta+\alpha_f-\alpha_r}{L}\right) \tag{9}$$

- Since β and u are slow-varying with respect to $\dot{\psi}$, terms $u\dot{\beta}\cos(\beta)$, $\dot{u}\sin(\beta)$ are widely negligible with respect to $u\dot{\psi}\cos(\beta)$ (corroborated by advanced simulations and experiments).

Linearization of (6) around $(\varphi_v, \dot{\varphi}_v) = (0,0)$ then leads to:

$$\ddot{\varphi}_{vL} = \frac{1}{h}\left[u^2\cos(\beta)\left(\frac{\delta+\alpha_f-\alpha_r}{L}\right) - \left(\frac{k_r\varphi_{vL}+b_r\dot{\varphi}_{vL}}{mh}\right)\right] \tag{10}$$

Since $u \approx v$ (as previously mentioned), the linear state-space model to be used in PFC algorithm is then:

$$\begin{cases} \dot{X} &= AX+Bw \\ Y &= CX \end{cases} \tag{11}$$

with the state-space vector $X = (\varphi_{vL}, \dot{\varphi}_{vL})^T$, the control variable $w = v^2$ and matrices:

$$A = \begin{bmatrix} 0 & 1 \\ \frac{-k_r}{mh^2} & \frac{-b_r}{mh^2} \end{bmatrix},\ B = \begin{bmatrix} 0 \\ \cos(\beta)\left(\frac{\delta+\alpha_f-\alpha_r}{hL}\right) \end{bmatrix},$$
$$C = \begin{bmatrix} 1 & 0 \end{bmatrix}$$

Based on Kalman criterion, the controllability of model (11) can be established provided that $\dot{\psi} \neq 0$. In other words, the linear roll angle φ_{vL} cannot be controlled when the vehicle is moving in straight line, which is quite natural. Then, close to neutral steering ($|\delta|$ below some steering limit), the PFC control algorithm is not activated and $v_{input} = v_d$.

C. Predictive maximum velocity computation

PFC algorithm is now applied to linear system (11) in order to derive the maximum velocity v_{max}. The principle of the predictive approach is summarized in Fig.4. Roughly, it consists in finding the control sequence which permits to reach "at best" the future set point after a specified horizon of prediction H.

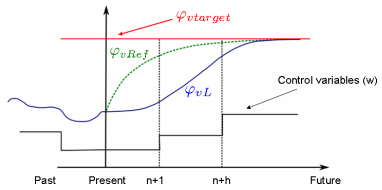

Fig. 4. Prediction principle.

More precisely, the algorithm consists in the following steps:

- The first step consists in computing the roll angle value, hereafter denoted $\varphi_{vtarget}$, leading to a *LLT* steady state value equal to the critical threshold LLT_{limit} chosen. Relying on the following assumptions: $\ddot{\varphi}_v = \dot{\varphi}_v = 0$ and $\xi_1 = (I_z - I_y)[\dot{\psi}^2\cos(\varphi_v)\sin(\varphi_v)]$ is widely negligible with respect to $\xi_2 = h\sin(\varphi_v)(F_{n1}+F_{n2})$ (in view of the mobile robot properties and actual conditions, the magnitude of ξ_1 stays beyond $100\sin(\varphi_v)$ while the magnitude of ξ_2 is at least equal to $3000\sin(\varphi_v)$) it can be derived from equations (7) and (8) that:

$$|LLT| = \left|\frac{F_{n1}-F_{n2}}{F_{n1}+F_{n2}}\right| \approx \left|\frac{2}{c}h\sin(\varphi_v)\right| \tag{12}$$

  As a result:

$$\varphi_{vtarget} = \pm\arcsin\left(\frac{cLLT_{limit}}{2h}\right) \tag{13}$$

- Next, a desired reference trajectory φ_{vRef}, joining the current state φ_{vNL} to $\varphi_{vtarget}$ during the horizon of prediction is defined. Typically a first order discrete system is considered:

$$\varphi_{vRef_{[n+i]}} = \varphi_{vtarget} - \gamma^i.\left(\varphi_{vtarget} - \varphi_{vNL_{[n]}}\right) \tag{14}$$

  The subscripts $[n]$ and $[n+i]$ (with $0 \leq i \leq h$) denote respectively the current time t and successive future time instants up to $t+H$ (since $[n+h]$ corresponds to time instant $t+H$) and γ is a parameter tuning the settling time for the reference trajectory to reach the set point.
- Then, at each sample time, an optimal control sequence $(w_{[n]},...,w_{[n+h]})$ bringing φ_{vL} to $\varphi_{vtarget}$ is computed

through the minimization of a quadratic criterion hereafter noted $D_{[n]}$. Moreover, since the linearization of equation (6) introduces some approximations that necessarily impair the accuracy of the predicted values of the roll angle and then of the LLT, the extended criterion $D_{[n]}$ incorporates the current and expected discrepancies between the roll angle values supplied by the nonlinear model (6) and the linear model (11):

$$D_{[n]} = \sum_{i=1}^{h} \left\{ \widehat{\varphi_{vL}}_{[n+i]} + \widehat{e}_{[n+i]} - \varphi_{vRef\,[n+i]} \right\}^2 \qquad (15)$$

where $\widehat{\varphi_{vL}}_{[n+i]}$ denotes the predicted output process obtained from linear model (11) and the control sequence and, where the future output error $\widehat{e}_{[n+i]}$ is defined as:

$$\widehat{e}_{[n+i]} = e_{[n]} = \varphi_{vNL_{[n]}} - \varphi_{vL_{[n]}}, \quad 1 \leq i \leq h \qquad (16)$$

The minimization can be achieved thanks to the decomposition of each element of the control sequence ($w_{[n+i]}$, $i \in [0,h]$) as a linear combination of base functions:

$$w_{[n+i]} = \sum_{k=1}^{n_B} \mu_{k_{[n]}} w_{Bk_{[i]}}, \quad 0 \leq i \leq h \qquad (17)$$

where $\mu_{k_{[n]}}$ are the coefficients supplied by the minimization of $D_{[n]}$, n_B is the number of base functions and w_{Bk} are the base functions, generally chosen as polynomials:

$$w_{Bk_{[i]}} = i^{k-1}, \quad \forall k \qquad (18)$$

If the optimal control sequence obtained from the minimization of $D_{[n]}$ was applied over the horizon of prediction, then φ_{vL} and LLT would reach respectively $\varphi_{vtarget}$ and LLT_{limit} at time $t+H$. Therefore, the first element of the control sequence, i.e. $w_{[n]}$, has to be considered as the maximum control input value, and then the maximum vehicle velocity at sample time $[n]$ is $v_{max} = \sqrt{(w_{[n]})}$. Finally, the PFC algorithm comprises two parameters to be tuned: the gain γ (specifying the shape of the reference trajectory) and the horizon of prediction H.

V. Experimental results

Since advanced simulation results, obtained with the predictive functional control law and a virtual quad bike, have already been presented in [5], this paper presents real experiment performed with the robot described in Fig. 5. It consists of an electric off-road vehicle, whose weight and maximum speed are respectively $350kg$ and currently $8m.s^{-1}$. The main exteroceptive sensor on board is a Dassault-Sercel dual frequency "Aquarius 5002" RTK-GPS receiver, which can supply an absolute position accurate to within $2cm$, at a $10Hz$ sampling frequency. In addition, a gyrometer supplying a yaw rate measurement accurate to within $0.1^\circ.s^{-1}$ is fixed on the chassis as well as a steering angle sensor and a Doppler radar. Finally, preliminary measurements and calibrations have supplied the following dynamic parameter set for this robot, to be reported in the algorithms:

Total mass	m =350kg
Yaw inertia	$I_z = 270\ kg.m^2$
Wheelbase	L=1.2m
Rear half-wheelbase	b=0.58m

TABLE I
Experimental robot dynamic parameters

Fig. 5. Experimental platform.

Then, with the experimental platform described above, a reference trajectory was manually recorded (in black dotted line in Fig.6): it is composed of a straight line connected smoothly to a curve with a constant $4.5m$ radius of curvature. The red line represents the real trajectory of the mobile robot, during a path following achieved with $v_d = 6m.s^{-1}$. As it can be seen, the integration of grip conditions in path tracking control law permits a high accurate result, since the error does not exceed $50cm$ (during transient phases). On the opposite, classical path tracking control algorithm (based on pure kinematic modeling) leads to largest errors in this context (more than $3m$), as reported in blue dotted line.

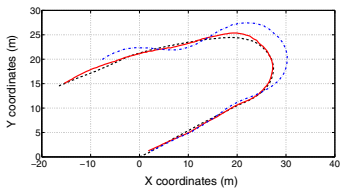

Fig. 6. Trajectory used to validate stability control.

More precisely, two tests have been performed: the first one consists in using path tracking control without predictive control and a constant $v_d = 6m.s^{-1}$ velocity. The second test consists in using the predictive functional control algorithm dedicated to LLT limitation with $v_d = 6m.s^{-1}$, $H = 1s$ (chosen according to the vehicle dynamic features), with 10 coincidence points (i.e. $h = 10$), $\gamma = 0.2$ and $LLT_{limit} = 0.35$. Fig.7 shows the time evolution of the measured velocity v_{m1} when path tracking is done without velocity control ($v_{m1} \approx v_d \approx 6m.s^{-1}$ after settling time) in black dash-dotted line, the maximum velocity v_{max} (computed with the PFC algorithm, in red solid line) and the rear axle velocity v_{m2} measured on the vehicle (in green dashed line) when velocity control is used. As described in Section IV-A, v_{m2} is supposed to be equal to the minimum of v_d and v_{max}. From $t = 0s$ to $t = 5.8s$, v_{m2} is equal to v_d. Then, between $t = 5.8s$ to $t = 9.2s$, during the curved part of the reference path, the velocity control variable applied to the vehicle is the maximum velocity given by the predictive functional control algorithm. However, due to the delay introduced by the velocity actuator, the measured velocity v_{m2} is satisfactorily

superposed with v_{max} only beyond $t = 7.8s$. Finally, after $t = 9.8s$, v_{max} is superior to the desired velocity, so that v_d can again be actually applied and after settling time ($t = 13s$), the measured velocity v_{m2} converges to v_d.

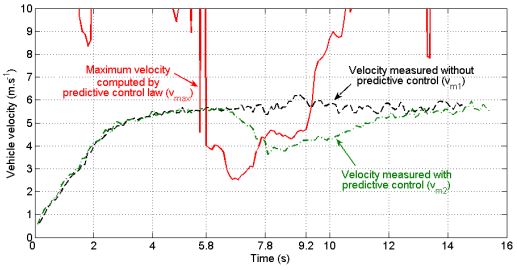

Fig. 7. Velocities comparison during real experiment.

Figure 8 shows the time evolution of the Lateral Load Transfer of the vehicle. LLT without prediction (LLT obtained when $v_{m1} \approx v_d$ is measured on the vehicle) is depicted in black dash-dotted line and the LLT measured with the predictive control is depicted in red solid line (LLT obtained with v_{m2}, i.e. when the minimum of v_d and v_{max} is applied to the vehicle). In this figure, the LLT obtained with v_{m1} is largely superior to LLT_{limit} fixed here at 0.35. On the contrary, after the settling time (after $t = 8s$), the LLT measured with v_{m2} satisfactorily converges to the LLT_{limit}. Indeed, between $t = 6s$ and $t = 8s$, the LLT measured is superior to the LLT_{limit}, since the velocity actuator introduces a delay between the velocity control variable, here equal to the maximum velocity v_{max} computed via PFC algorithm and the real velocity of the vehicle v_{m2}, as explained in the previous paragraph and which can be seen on Fig.7. Finally, when $v_{m2} \approx v_{max}$, the LLT measured is equal to 0.35.

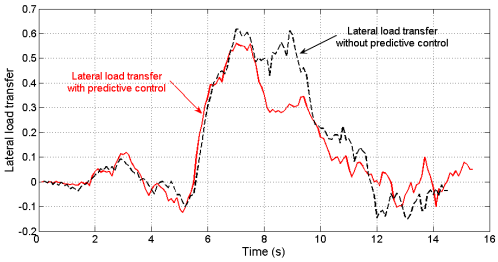

Fig. 8. Lateral Load Transfer measured.

VI. Conclusion

This paper proposes a new safety device, based on Predictive Functional Control formalism, dedicated to off-road mobile robots operating on a natural and slippery ground. First, previous work on path tracking control, built from both adaptive and predictive control laws, has been recalled. Sliding effects have been taken into account according to a mixed kinematic and dynamic observer adapting on-line the tire cornering stiffnesses of the front and rear tires. It enables to take into account the non-linear behavior of the tire and the variations in grip conditions when computing the sideslip angles. Then, these sliding parameters are introduced into a predictive functional control law, based on a vehicle dynamic model, so as to compute the maximum velocity admissible by the robot, ensuring that the *LLT* indicator never exceeds the rollover threshold (i.e. $|LLT| \leq LLT_{limit}$). Real experiments, carried out with a high speed mobile robot, demonstrate the applicability and the relevancy of the proposed control strategy to avoid rollover situations and ensure path tracking trajectory.

Future work will be dedicated to reduce the delay introduced by the velocity actuator. Indeed, it has been highlighted that the velocity measured on the vehicle differs from the velocity control variable. Therefore, another predictive control law based on the velocity actuator characteristics is under development so as to eliminate the delay.

References

[1] J. Ackermann and D. Odenthal. Advantages of active steering for vehicle dynamics control. In *International Conference on Advances in Vehicle Control and Safety*, Amiens: France, 1998.

[2] R. Bosch. *Safety, comfort and convenience systems*. Wiley, Hoboken, U.S.A., 2006.

[3] N. Bouton, R. Lenain, B. Thuilot, and J-C. Fauroux. A rollover indicator based on the prediction of the load transfer in presence of sliding: application to an all terrain vehicle. In *Intern. Conf. on Robotics and Automation*, pages 1158–1163, Roma, Italy, 2007.

[4] N. Bouton, R. Lenain, B. Thuilot, and P. Martinet. A rollover indicator based on a tire stiffness backstepping observer : Application to an all-terrain vehicle. In *Int. Conf. on Intelligent RObots and Systems (IROS)*, Nice, France, 2008.

[5] N. Bouton, R. Lenain, B. Thuilot, and P. Martinet. An active anti-rollover device based on predictive functional control : Application to an all-terrain vehicle. In *Int. Conf. on Robotics and Automation (ICRA)*, Kobe, Japan, 2009.

[6] P. Gaspar, Z. Szabo, and J. Bokor. The design of an integrated control system in heavy vehicles based on an lpv method. In *44th IEEE Conf. on Decision and Control (CDC)*, pages 6722–6727, Seville, Spain, 2005.

[7] R. Lenain. *Contribution à la modélisation et à la commande de robots mobiles en présence de glissement*. PhD thesis, Université Blaise Pascal, Clermont II, 2005.

[8] R. Lenain, B. Thuilot, C. Cariou, and P. Martinet. Multi-model based sideslip angle observer : Accurate control of high-speed mobile robots in off-road conditions. In *Int. Conf. on Intelligent RObots and Systems (IROS)*, Saint Louis, U.S.A., 2009.

[9] A.J.P. Miège and D. Cebon. Design and implementation of an active roll control system for heavy vehicles. In *6th Int. symposium on Advanced Vehicle Control (AVEC)*, Hiroshima, Japon, 2002.

[10] National Highway Traffic Safety Administration (NHTSA). Trends in static stability factor of passengers cars, light trucks and vans. Technical report, U.S. department of transportation, 2005.

[11] H. B. Pacejka. *Tire and vehicle dynamics*. Society of Automotive Engineers, 2002.

[12] E.G. Papadopoulos and D.A. Rey. A new measure of tipover stability margin for mobile manipulators. In *Inetrn. Conf. on Robotics and Automation*, pages 3111–3116, Minneapolis, U.S.A., 1996.

[13] J. Richalet. Industrial applications of model based predictive control. *Automatica*, 29(5):1251–1274, 1993.

[14] J. Richalet, E. Abu, C. Arber, H. Kuntze, A. Jacubasch, and W. Schill. Predictive functional control - application to fast and accurate robots. In *10th IFAC World Congress*, Munich, Germany, 1997.

[15] P. Sardain and G. Bessonet. Forces acting on a biped robot. center of pressure - zero moment point. *IEEE Transactions on systems, man, and cybernetics*, 34(5):630–637, 2004.

[16] B. Schofield, T. Hagglund, and A. Rantzer. Vehicle dynamics control and controller allocation for rollover prevention. In *International conference on control applications*, Munich, Germany, 2006.

[17] R. Siegwart and I.R. Nourbakhsh. Introduction to autonomous mobile robots. *MIT Press*, 2004.

[18] J. Stéphant. *Contribution à l'étude et à la validation expérimentale d'observateurs appliqués à la dynamique du véhicule*. PhD thesis, Université de Technologie de Compiègne (UTC), 2004.

[19] A. Vivas and V. Mosquera. Predictive functional control of a PUMA robot. In *Proc. of the first ICGST International Conference on Automatic Control and Systems Engineering (ACSE)*, pages 35–40, Cairo, Egypt, 2005.